Functional Imaging of Autoregulation

Randall L. Barbour[1,2], Yaling Pei[2], Mark Farber[1], Harry L. Graber[1,2], Yong Xu[1,2] and Deepak Sreedharan[1]
[1]*Dept. of Pathology / SUNY Downstate Medical Center / 450 Clarkson Ave. Brooklyn, NY 11203; yong.xu@downstate.edu*
[2]*NIRx Medical Technologies LLC / 15 Cherry Lane / Glen Head, NY 11545*

INTRODUCTION

Central to any imaging method are contrast features. By exploring the action that variations in biological states have on naturally occurring or injected contrast agents, functional imaging techniques can potentially explore a much broader class of phenomenology than structural methods. An especially interesting one is associated with autoregulation. This is the process whereby, through various feedback mechanisms, tissues self-regulate their environment to maintain homeostasis. The particulars of these influence virtually all aspects of intermediary metabolism, and disruptions lead to a multitude of disease states (*e.g.*, autonomic, vascular, endocrine, *etc.*). Despite this general understanding, strategies well suited to explore this rich phenomenology have not yet been developed. While here we demonstrate imaging of a specific class of autoregulation, *i.e.*, vascular autoregulation, the approach taken is completely general, and in principle can be extended to any element of intermediary metabolism or higher-order mechanisms associated with this process.

Key to our approach is appreciation for the importance of studying contrast variations that are tied to feedback mechanisms. Also critical is that the feedback process itself leads to contrast variations that can go undetectable without adopting specific attributes related to data collection and processing. Specifically, we recognize the need to: (i) adopt acquisition speeds fast compared to the relevant phenomenology, and (ii) organize the data in a manner consistent with the feedback processes themselves.

As an example, Table 1 delineates the process of vascular autoregulation into six states that are experimentally definable using functional diffuse optical tomography (fDOT). The considered delineation recognizes three principal elements tied to this process: states of oxygen balance (1 and 4); uncompensated imbalance (2 and 5); and compensated imbalance (3 and 6). While these are generally appreciated, the fact that within a specific Hb class (*i.e.*, oxyHb, deoxyHb, totalHb) they have opposite algebraic signs indicates that summation of these, which is the usually practice, will render individual features, several of which are associated with physiological triggers, undetectable.

METHODS

Data Collection:

Experimental data were collected using a NIRx DYNOT Model 232 imager fitted with either a limb or breast measuring head. Dual wavelength optical measurements were performed using a fast time multiplexing scheme with parallel detection. Limb studies employed a 24 S x 24 D circular array; breast 31 S x 31 D array.

Image Reconstruction:

Optical data were preprocessed by applying a low pass filter (0.15 Hz), normalized to baseline, and evaluated using the Normalized Difference Method described by Pei et al. (2001). Image operators were computed by solving the diffusion equation using Robin boundary conditions. This produces a time series of 2D or 3D images that are robust to many of the uncertainities of experiment.

Autoregulatory State (AS) Calculation

Having computed a normalized image time series, the time dependent pixel responses were scored as to which of the six states identified in Table 1 they correspond to. Three basic measures of interest were explored:

1. Time dependent spatial mean of the partial volume of identified AS states.
2. Spatial maps of the AS states.
3. Spatial maps that identify the fractional time spent in each AS state.

The Autoregulatory Cycle: Table 1 lists the different autoregulatory states that result from efforts to maintain a supply-demand balance in oxygen delivery to tissue. Here we consider State 1 and 4 as representing conditions of relative balance as neither a condition of oxygen debt or excess is present. A continued decline in totHb from State 1 (or sudden rise in demand) can result in induced oxygen debt (State 2). This can trigger a vasodilatory response (State 3) enhancing oxygen delivery. With continued dilation a state of balance is restored (State 4). Progression to State 5 occurs should the extent of oxygen debt be sufficient to trigger a reactive hyperemia (usual case). Excess supply triggers a vasoconstriction (State 6) which with continued decrease returns to State 1.

Hemoglobin State	State 1	State 2	State 3	State 4	State 5	State 6
Hb_{oxy}	-	-	-	+	+	+
Hb_{deoxy}	-	+	+	+	-	-
Hb_{tot}	-	-	+	+	+	-
	Balanced	Uncomp. oxygen debt	Comp. oxygen debt	Balanced	Uncomp. oxygen excess	Comp. oxygen excess

Table 1. Hb states paired according to Hb dependence on autoregulation.

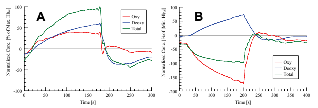

Figure 1. Time dependence of integrated Hb signal to venous congestion (A) and cuff ischemia (B).

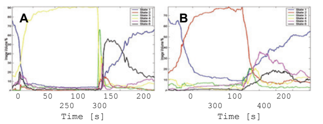

Figure 2. Time-dependence of volume fraction of Hb autoregulatory states to venous congestion (A) and cuff ischemia (B).

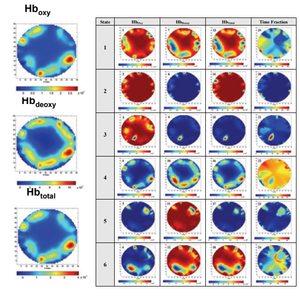

Figure3. Left. Cross sectional images of forearm with venous congestion. Right. Corresponding AS and time fraction maps.

Clinical Study

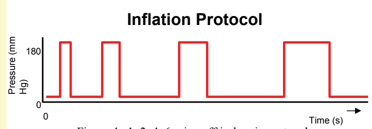

Figure 4. 1, 2, 4, 6 min cuff ischemia protocol.

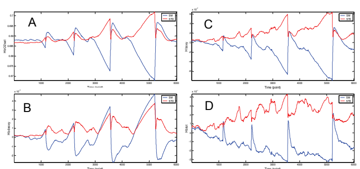

Fig. 5 Response to protocol in Fig 4. A, HbO2Sat, B. OxyHb, C, DeoxyHb, D, TotHb.

Healthy Control: 43-yr-old Asian Male, Arterial Ischemia

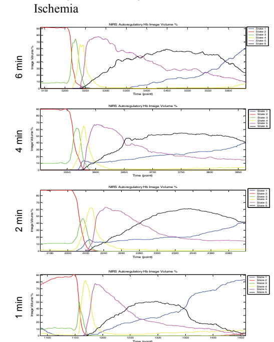

Fig. 6 AS states from Fig 5.

Impaired Glucose Tolerance: 67-yr-old African-American Male

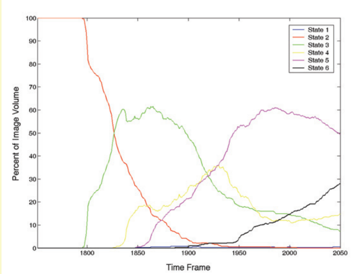

Fig. 7 AS recovery time course.

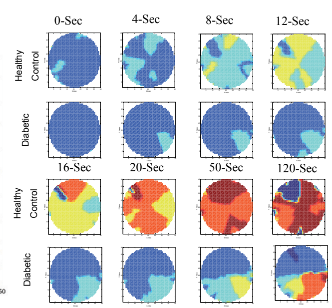

Figure 8. Image time course of recovery from ischemia.

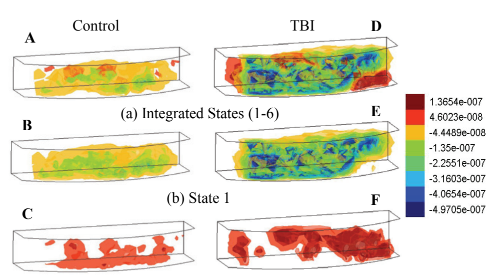

Figure 9. Volume rendered images of total Hb for integrated (a), State 1, (b) and State 4, (c) phase of the autoregulatory response.

RESULTS

Results in Figure 1 shows the temporal response of the hemoglobin signal (time-dependent spatial mean) obtained from the forearm to inflation of a pneumatic cuff to 60 and 180 mm Hg. The latter produces venous congestion marked by a rise in the tissue blood volume without significant Hb desaturation. In contrast, the former produces a prompt desatuation of Hb, which undergoes rapid recovery upon reperfusion with accompanying reactive hyperemia. These responses are well appreciated by many.

Results in Figure 2 show the identical data except categorized according to Table 1 and expressed as a time dependent partial volume associated with each AS state. Inspection reveals that these maneuvers produce the expected State changes (State 4 with venous congestion, State 2 with cuff ischemia). Notably, upon release of the cuff we see in both cases a rapid progression through each of the successive AS states with a more prolonged recovery times associated with ischemia.

The spatial dependence of the AS state response to the venous congestion maneuver is shown in Figure 3. For comparison we also show the integrated Hb state response (usual way of expressing NIRS results). Comparison shows that a wealth of additional contrast features are identified in the AS state images. Also shown are maps of the computed time fraction associated with each AS state.

Figure 4 outlines the inflation protocol used in a clinical study designed to explore the effects of age and distrubances in carbohydrate metabolism on the AS response. Figures 5 and 6 compares the response seen in the integrated Hb signal to the AS profile. Inspection reveals a titratable response in State 3 with a decline in State 4 levels.

For comparison, shown in Figures 7 and 8 and corresponding responses seen in representative individuals with impaired carbohydrate metabolism. Seen is a delayed recovery response especially in the individual with diabetes.

AS Response in TBI

To further explore the utility of examining the AS response as outlined here we have examined subjects with TBI. Forehead measurements were made using a 10 x 3 array (30 S x 30 D) and subjects were ask to perform an N-Back test. For illustrative purposes we show results from one individual (see 145 W-AM) with TBI compared to healthy control. Most evident is a large increase in the amplitude of State 1 and 4 for the TBI subject suggesting that regions of hypo and hyperperfusion exist.

CONCLUSIONS

Time-series imaging of experimentally measurable categorical states associated with feedback mechanisms provides a basis of exploring autoregulatory phenomena in significantly greater detail than previously recognized. Here we have explored measures available from the study of the hemoglobin signal. In principal the considered approach is completely general and can be extended to explore wide range of autoregulatory phenomena given the availability of suitable contrast agents.

ACKNOWLEDGMENTS

Support by the National Institute of Neurological Disorders and Stroke (R41 NS050007-01) is gratefully acknowledged.